Journal of Wood Science

ORIGINAL ARTICLE

Open Access

Quantitative evaluation of unique residual stress observed in Japanese zelkova (*Zelkova serrata*) trunk

Naohisa Kameyama[1], Miyuki Matsuo-Ueda[2*], Shuoye Chen[3], Zhuoting Jiang[1], Fabio M. Yamaji[4], Joseph Gril[5], Masato Yoshida[1] and Hiroyuki Yamamoto[1*]

Abstract

This study proposed a method to quantify the unique patterns of longitudinal residual stress in large-diameter Japanese zelkova (*Zelkova serrata*) logs and evaluated their characteristics using 11 logs from 8 trees. While the lateral distributions of longitudinal residual stress show the smooth bell curve patterns in many other species, those of Japanese zelkova logs often exhibit a unique and varied zigzag pattern, as if they had "spikes" along their lateral distribution. The study defined an index called "spike level" to quantify the intensity of spike-shaped strains that deviate from the expected trend of the lateral distribution. The following key findings were obtained through the quantification procedure and investigation of the spike level: 1) Each residual stress distribution was composed of two components: a global distribution that made a smoother distribution, and local stresses that made spikes on the distribution. 2) The index "spike level" varied widely among the samples and reflected well the deviation from the smooth bell curve pattern. 3) The residual stress distribution showed three-dimensional complexity and was not axially symmetric around the pith. This quantification method enables comparison between logs and provides a foundation for further research on the unique residual stress patterns in Japanese zelkova, including the mechanisms of its formation and its impacts on wood processing.

Keywords Keyaki, Large-diameter, Growth stress, Hardwood

*Correspondence:
Miyuki Matsuo-Ueda
matsuo.miyuki.4d@kyoto-u.ac.jp
Hiroyuki Yamamoto
hiro@agr.nagoya-u.ac.jp
[1] Graduate School of Bioagricultural Sciences, Nagoya University, Chikusa, Nagoya 464-8601, Japan
[2] Graduate School of Agriculture, Kyoto University, Kitashirakawa Oiwake-Cho, Sakyo-Ku, Kyoto 606-8502, Japan
[3] Research Institute for Sustainable Humanosphere, Kyoto University, Gokasho, Uji 611-0011, Japan
[4] Department of Environmental Sciences, Federal University of São Carlos (UFSCar), Campus of Sorocaba, Rodovia João Leme Dos Santos, Km 110, Sorocaba, SP, Brazil
[5] INRAE, PIAF, CNRS, Institut Pascal, Université Clermont Auvergne, Campus des Cézeaux, 2 av. Blaise Pascal, Aubière cedex 363178, France

Introduction

Japanese zelkova (*Zelkova serrata*, "keyaki" in Japanese) is a representative hardwood tree that grows in a variety of environments, including natural forests, gardens, and along streets. Japanese zelkova grows into large-diameter trees, making them well suited for the production of large-diameter timber [1–3]. Japanese zelkova wood is characterised by its high mechanical properties and distinct grain. For these reasons, it has traditionally been used in architecture and furniture making and remains a highly valued timber.

As mentioned above, Japanese zelkova wood has been used traditionally for a long time. Determining its quality, however, has relied on subjective judgments by experts. Therefore, the authors initiated a series of projects to scientifically elucidate the properties of Japanese zelkova wood, from standing trees to final utilisation. Within this, measurements were first started on residual stresses [4], which are known to cause deformation during sawing.

Generally [5], the distribution of longitudinal residual stress along the radial direction in a typical upright tree has a smooth bell shape, and the compressive stress reaches a maximum near the pith, mechanical neutrality (zero) at a distance of approximately two-thirds of the radius from the pith, and the tensile stress increases toward the bark. Many studies using enough numbers of tree samples or various wood species reported the bell-shaped typical distribution of residual stress; over 200 trees of eucalyptus (*Eucalyptus gigantea*) [6], 202 and 86 trees of beech (*Fagus silvatica*) in [7] and [8], respectively, 63 trees of Japanese cedar (*Cryptomeria japonica*) [9]; Japanese cypress (*Chamaecyparis obtusa*) [10], Japanese larch (*Larix* sp.) [11], Japanese blue oak (*Quercus glauca*) [10], Japanese beech (*Fagus crenata*) [12], mangium (*Acacia mangium*) [13], falcata (*Paraserianthes falcataria*) [14], and teak (*Tectona grandis*) [15]. The released strain of the residual stress has been used as a good indicator of the stress distribution [9]–[15]; hereafter, the released strain is used to discuss the characteristics of the residual stress.

However, Kameyama et al. [4] recently reported that the unique released strain distribution of Japanese zelkova logs exhibited zigzag patterns that often deviated from a smooth curve and typical bell shape. These patterns were characterised by spike-shaped released strains (hereafter, "spike-shaped strain") and suggested the presence of large, localized stresses (hereafter, "spike stress"). The entire shape of the released strain distribution was qualitatively classified into two patterns: "bell shape" and "not bell shape". For each, the appearance of the spike-shaped strain was classified into two categories: the spike-shaped strain presenting "throughout" and "partially" along the radial direction. Furthermore, the spike stress was found to be a localised stress that affected only a limited section along the longitudinal direction of the log rather than its entire length. These characteristics are completely different from those previously reported for other wood species. Okuyama et al. [11] showed a released strain distribution of Japanese zelkova, exhibiting similar unique trends as a single measurement example, but the study did not mention the particular characteristics of Japanese zelkova.

Kameyama et al. [4] established the methodology for the correct measurement of the Japanese zelkova characteristics with less experience than ever, and confirmed its characteristics –the zigzag patterns and spike-shaped strains– with a large number of logs. Consequently, the spike-shaped strains have not yet been quantified, and the characterization was still qualitative. It is useful to quantitatively evaluate its residual stress distribution to investigate the deformation such as heart shake and end split due to the release of stress during tree felling or log sawing which often occur on site, as well as to reveal the mechanism of the unique residual stress generation of Japanese zelkova from the viewpoint of tree biomechanics.

This study aimed to quantify spike-shaped strains that are thought to be caused by the release of spike stress by defining the intensity of spike-shaped strain as "spike level" to enable the quantitative comparison among test logs, and finally discussed the characteristics of the released strain distribution of Japanese zelkova. The quantification method was established based on a comparison with the typical released strain of Japanese cedar to consider the localised stress of Japanese zelkova.

Materials and methods

Materials

Eight Japanese zelkova trees were used to obtain logs for testing. These logs had a top-end diameter of about 45 cm or more and were called "Large-diameter logs". Four trees from Tochigi Prefecture were the same trees measured in the previous report [4], and four were newly harvested from Gifu Prefecture (Table 1). Two logs were obtained from each tree in Gifu Prefecture, except for one log that had a large hollow inside. Eleven logs in all were obtained at two harvesting sites, Gifu and Tochigi Prefectures, and then immediately transported to a sawmill, Morijitsu Mokuzai Kogyo Ltd. in Kakamigahara, Gifu. They were then wrapped with plastic waterproof sheets to minimize changes in moisture content until sawing. Then, the sawing of the diametral planks from the logs and the measurements of the released strain were conducted on the same day. From the tree harvesting to the measurements, the processes were completed within three months during the cold season (Table 1, "Date of residual stress measurement" and "Date of harvesting"). From this sample condition and the preliminary monitoring of the moisture content of other logs, it was expected that the moisture content of the samples was above the fibre saturation point.

Preparation of diametral planks and measurement of released strain of residual stress

Diametral planks containing pith and radial surfaces were obtained from the logs to measure the released strain of the residual stress in the longitudinal direction. Although the upright trees were chosen, when the tree trunk was slightly inclined in a growing state, the sawing position was set such that the planks contained both the upper and lower sides of the inclined trunk (Fig. 1a). For three sample trees (T5, 7, and 8), planks

Table 1 Information of diametral planks of 11 logs obtained from 8 standing trees (* T6-1 had a hollow trunk and was not used.)

Tree No	Growing site (Prefecture)	Ground	Log and plank No	Log position in tree	Plank width Top/middle/bottom (cm)	Plank length (cm)	Date of harvesting	Date of residual stress measurement
T1	Tochigi	Flat	T1		- / 62.5 / -	201	November 18th to 20th, 2019	January 28th to 29th, 2020
T2			T2		- / 89.0 / -	202		
T3			T3		- / 76.0 / -	248		
T4			T4		- / 78.0 / -	196		
T5	Gifu	Slope	T5-1	bottom	63.5 / 60.0 / 58.1	428	December 7th to 11th, 2022	February 28th to March 1st, 2023
			T5-2	top	48.0 / 47.5 / 43.0	471		
T6			T6-1*	bottom	–	–		
			T6-2	top	52.5 / 51.5 / 51.6	422		
T7			T7-1	bottom	65.0 / 63.8 / 62.0	403		
			T7-2	top	52.4 / 54.0 / 50.7	420		
T8			T8-1	bottom	58.6 / 55.0 / 54.5	401		
			T8-2	top	52.5 / 48.8 / 53.5	479		

of the top-side log were sawn orthogonally to those of the bottom-side logs (Fig. 1b). After sawing the diametral planks using a band saw (Fig. 2a), the plank surface was finished with an electric planer to ensure a uniform thickness of 5 cm and smooth the measurement surface. The widths and lengths of the planks are listed in Table 1. A surface closer to the pith was used as the measurement surface.

The strain "measurement position" was set at the line drawn transverse to the longitudinal direction at the centre of the plank (Fig. 3A). Strain gauges were pasted at 2-cm intervals from the pith to the bark sides (Figs. 2b and 3B). Each point of the strain gauges was defined as a "measurement point". The distance from the pith to each measurement point was expressed as r, with a pith of $r=0$ cm.

After obtaining the initial strain values, both ends of the plank were repeatedly crosscut by 10 cm in length ("1", "2", "3", ...in Fig. 3C) by a electric circular saw until approaching approximately 1 cm from edges of the strain gauges (hereafter, "gauge-edge line") (Fig. 2c, d and Fig. 3D). The released strains were measured at each crosscutting, and the change in the strain was examined as the distance between the measurement position and the crosscut position (l, Fig. 3E) decreased. Strain gauges (Kyowa Electronic Instruments KFGS-10–120-C1-11 L3M3R and L5M3R, three-wired, gauge length of 10 mm, cable lengths of 3 and 5 m), cyanoacrylate quick-setting glue (Kyowa Electronic Instruments CC-33A), and data-correcting units (Kyowa Electronic Instruments UCAM-65C-AC, EDX-10B, EDX-14A, and DBS-120B-8) were used.

Results and discussion

Change in released strain distribution through the crosscutting process

Figure 4 illustrates the boards crosscut at the representative l values (upper row) and the corresponding changes in the radial distribution of the longitudinal released strain (lower row). Focusing on the changes in the shape of the released strain distribution, the distribution initially maintained a smooth bell shape ($l=\sim 20$ cm). However, spike-shaped strains appeared when the plank was crosscut at $l=10$ cm and became sharper at the gauge-edge line, as reported in a previous study [4].

Figure 5 shows the changes in the released strain at each measurement point (Fig. 5a, c, and e) and the changes in the radial distribution of the released strain of the same sample plank (Fig. 5 b, d, and f), comparing Japanese zelkova with Japanese cedar measured using the same method [16]. In the case of Japanese cedar (Fig. 5a and b), the strain values remained zero from $l=200$ cm to $l=80$ cm, then increased or decreased until l reached the gauge-edge line. Spike-shaped strains did not appear at all, and the released strain monotonously increased or decreased with decreasing l value. In the case of Japanese zelkova (Fig. 5c and d), the strain values remained zero from $l=200$ cm to $l=120$ cm. When I reached 110 cm, the strain values started to monotonously change until l was approximately 30 cm. The radial distribution of the released strain maintained a bell shape, where l was between 30 and 110 cm. When l was less than 20 cm, the strain values at each point changed differently with decreasing l; the values decreased or increased regardless of the previous trend, producing a spike-shaped

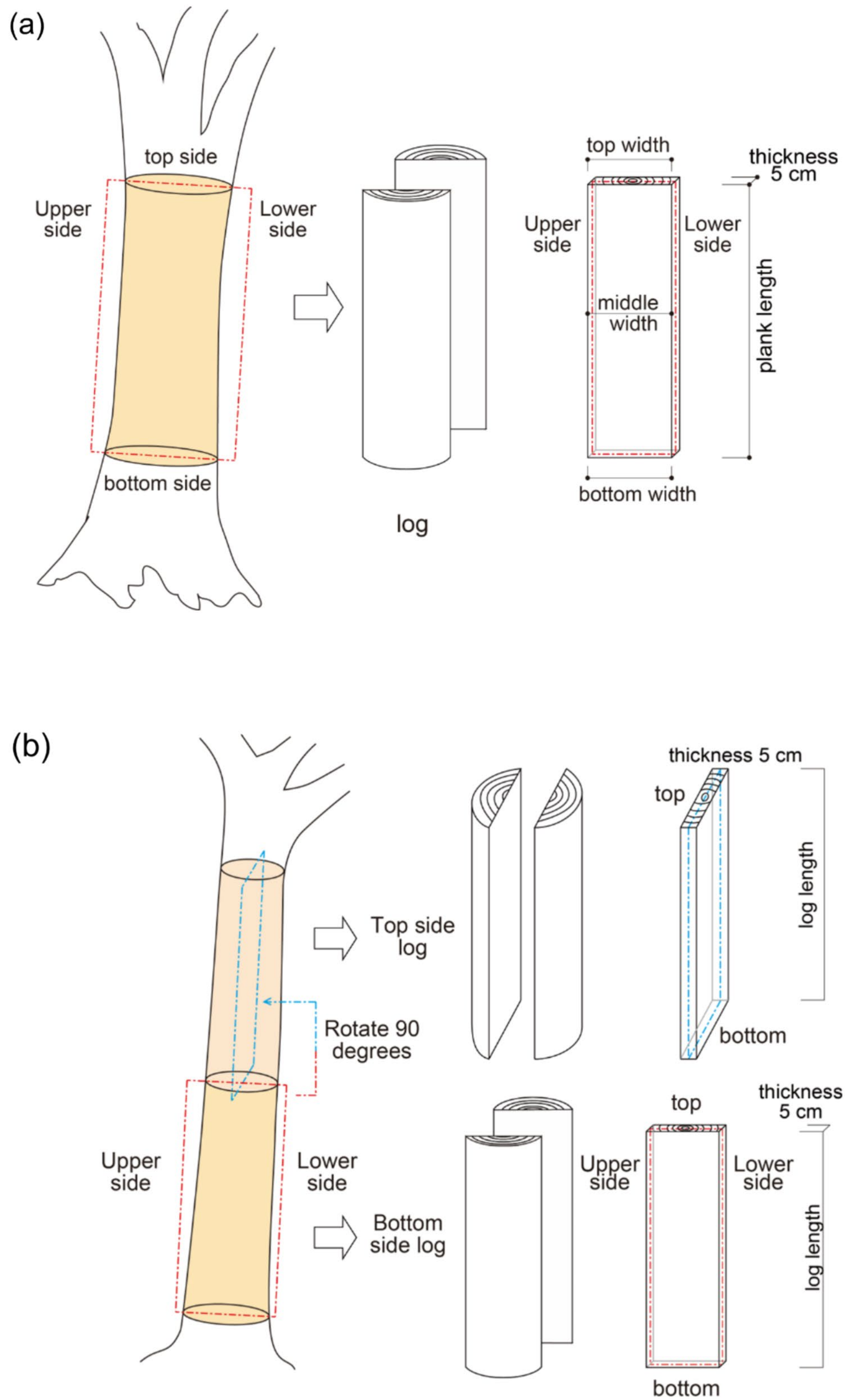

Fig. 1 Sampling geometry of diametral planks. **a** Preparation of a diametral plank from a standing tree (T1–T4). **b** Preparation of two diametral planks from a standing tree (T5–T8)

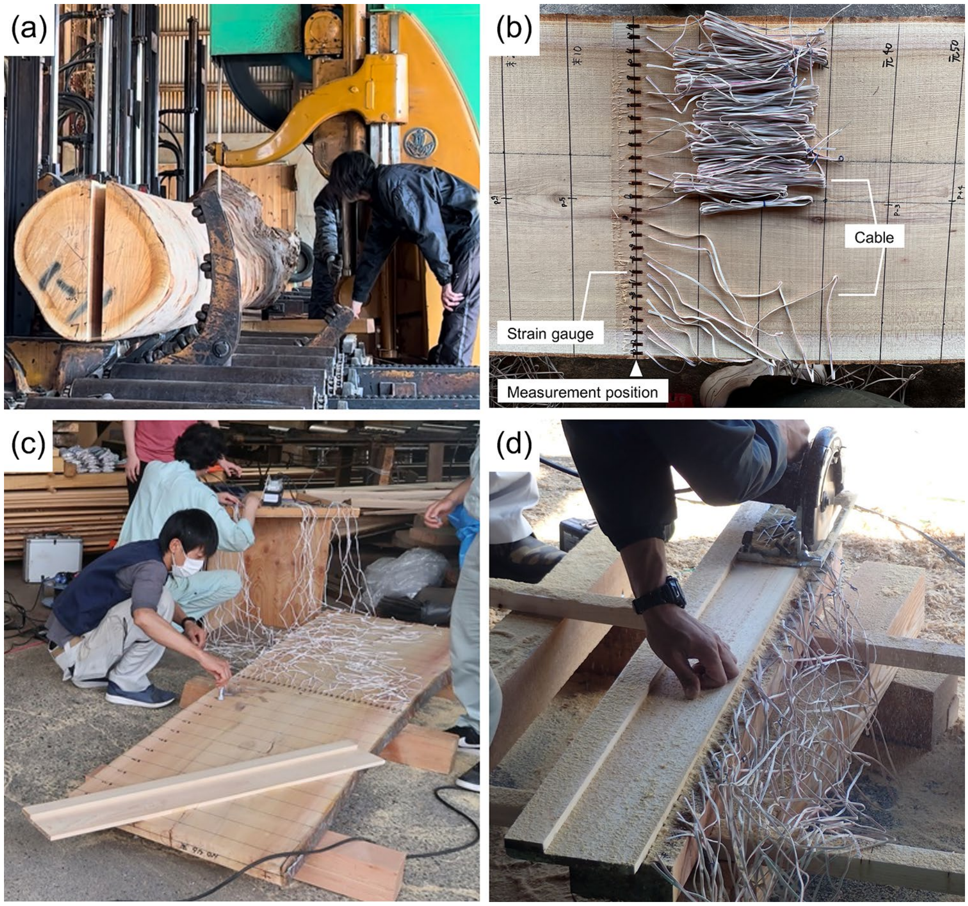

Fig. 2 Sawing process of diametral planks and measurement of released strain. **a** Sawing of diametral plank. (**b**) and (**c**) Diametral plank with strain gauges attached to the measurement surface. **d** Crosscutting of the plank at the gauge-edge line

strain distribution. The regions where l was between 0 cm (= gauge-edge line) and 20 cm and between 30 and 110 cm were named as "local area" and "global area", respectively, to express the areas where spike-shaped strain did/did not appear. Turning back to Fig. 5a, the evolution of residual stress of Japanese cedar can be said to have only the global area. In summary, the residual stress in the local area exhibiting the spike stress which characterized the distribution of Japanese zelkova, whereas the residual stress distribution in the global area was not influenced by spike stress and maintained a smooth bell shape.

Quantification of spike-shaped strain

As shown in Fig. 5a and b, in the case of large-diameter Japanese cedar, the released strain distribution maintained a bell shape up to the crosscut at the gauge-edge line, with a monotonous change in the strain values with decreasing l. Conversely, for Japanese zelkova, the evolution of the strain was similar to Japanese cedar in the global area, while the evolution in the local area led to the spike-shaped strain, making zigzag patterns in the released strain distribution. To quantify the spike stress observed in the local area, it seemed effective to assess the deviation from the trend in the global area, under the assumption of a continuous change without the emergence of spike stress up to the gauge-edge line. This method demonstrates that the Japanese zelkova pattern is formed by the numerical synthesis of a standard bell-shaped distribution and spikes. Furthermore, it enables future discussion linking the origin of spike strain to anatomical features—especially, tension wood, interlocked grain, and vessel distribution.

Based on this assumption, the following concepts were used to define an index that represents the intensity of the spike-shaped strain.

– Assuming that spike-shaped strains would not appear in Japanese zelkova, the released strain should evolve linearly from the global area to the gauge-edge line, similar to that in Japanese cedar.

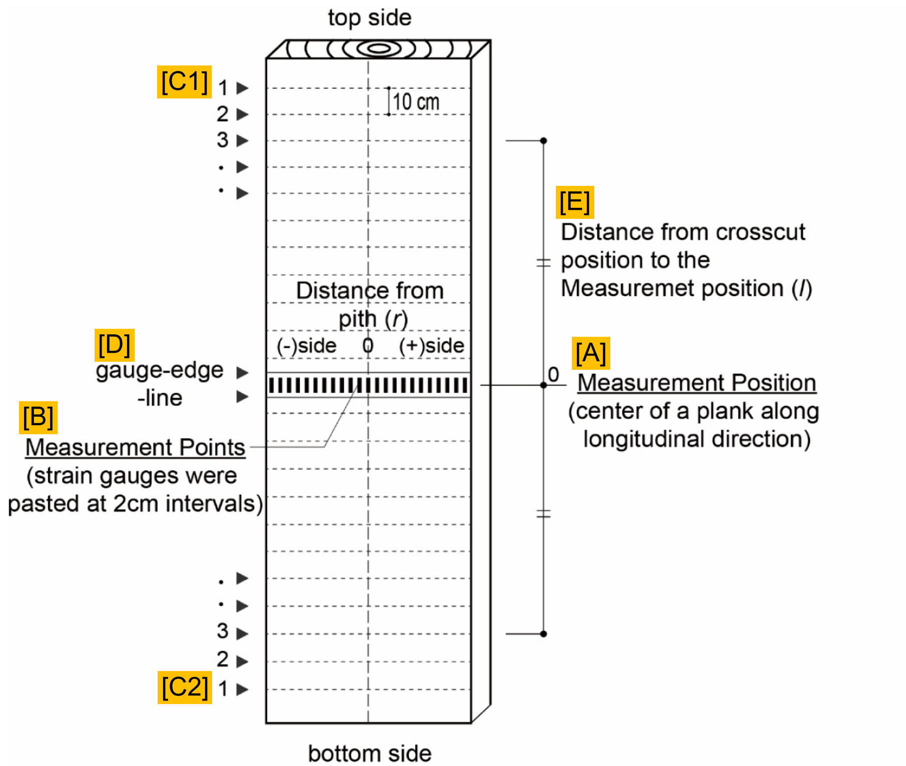

Fig. 3 Definition of the distance from the pith (*r*) and the distance from the crosscut position to the measurement position (*l*). Strain gauges were pasted at the centre of the plank. Both ends of the plank were crosscut every 10 cm, and the released strain was measured at each crosscut until the gauge-edge line. [A]–[E] correspond to the main text

– However, spike-shaped strains actually appear in the local area of Japanese zelkova, deviating from the trend in the global area.
– The intensity index of the spike-shaped strain can be defined as the difference between the actual spike-shaped strain and the virtual strain estimated at the gauge-edge line, assuming that the spike-shaped strain does not appear and the trend in the global area continues up to a gauge-edge line.

Based on the above concepts, the calculation of the index at each measurement point can be explained as follows with the aid of Fig. 5e and f. Fig. 5e extracted the strain evolution curve of a measurement point at $r = -10$ cm from Fig. 5c. Fig. 5f extracted the measured distribution at the gauge-edge line from Fig. 5d and describes the extrapolated distribution that is calculated in the following way. In the relationship between the released strain and l (Fig. 5e), the regression line in the global area was extrapolated toward the local area, and the extrapolated strain value at $l = 0$ cm was calculated (for example, 671 μs at $l = 0$ cm, in Fig. 5e). This extrapolated strain values were calculated for all the measurement points, as a result, the distribution of the extrapolated strain values against distance from the pith was obtained (Fig. 5f, "extrapolated"). The distribution of the extrapolated strain value had a smooth bell shape. The absolute difference between the extrapolated value and the measured value, $|y(r)|$, was then calculated for each measurement point. As an example of $|y(r)|$, $|y(-10)|$ is indicated in Fig. 5f, showing the difference between the extrapolated value and the measured value. The absolute difference $|Y|$ between the maximum and minimum values of the extrapolated distribution was also calculated. The $|y(r)|$ divided by $|Y|$, namely, normalized $|y(r)|$, was defined as the "spike level", $SL(r)$, which represented the intensity of the spike strain at each measurement point. The $SL(r)$ potentially ranged from 0 to 1, and the higher the $SL(r)$ was, the larger the spike strain was. The average value of $SL(r)$ for all r was obtained for each plank, defined as "individual spike level", ISL, representing how each plank had intense spikes.

Evaluation of released strain distributions with spike level

Figure 6 shows the distributions of the measured strain and extrapolated strain normalised by $|Y|$ to compare among sample planks, as well as the distribution of $SL(r)$ as green bars and ISL values for all sample planks. The

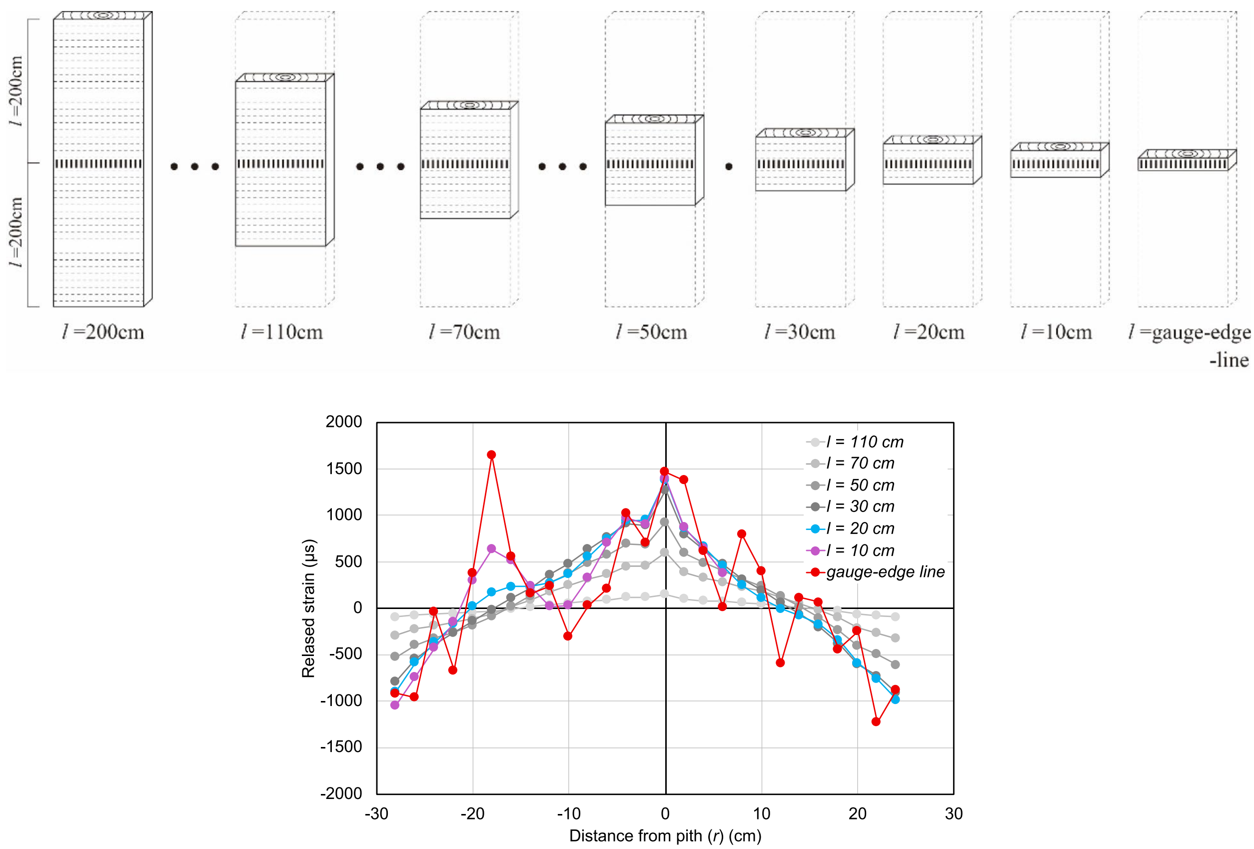

Fig. 4 A diametral plank crosscut at different *l* and corresponding changes in released strain distribution during the crosscutting process (example of the sample T8). Upper: Illustration of each crosscut at a different *l*. Lower: released strain distribution when the plank was cut at each *l*

quantification with $SL(r)$ seemed successful since when the deviation of measured strain from extrapolated strain was larger, $SL(r)$ values also became larger. The planks were categorised based on the distribution shape as “bell shape” and “not bell shape” and by the *ISL* value as low, middle, and high. To compare top and bottom side logs, the category “top side log” was also added.

The *ISL* values, ranging from 0.06 to 0.28, were extremely high for two non-bell-shaped distributions (T2 and T3), whereas the *ISL* was generally lower in bell-shaped distributions, especially in some planks where the measured distribution closely matched the extrapolated distribution (T5 and T7). *ISL* was higher in the top-side logs when comparing the top and bottom-side logs of T5, T7, and T8, which was attributed to the fact that the top-side logs, being closer to branching, were more affected by bending moments induced by the branch weight. The testing planks were sawn, avoiding the branching parts as much as possible, but the extent to which the branching pattern mechanically affects the residual stress in the trunk has not been clear. Further investigation, including the whole tree shape, is required to fully address this issue.

The extrapolated distribution can be considered as the virtual residual stress state along the entire longitudinal direction, including the local spike stresses at any different position on the entire plank. When the extrapolated distribution was bell-shaped, the entire stress distribution was balanced, similar to other typical wood species, but locally disturbed by the spike stresses. On the other hand, it was supposed that the extrapolated distribution of not bell-shaped and in higher *ISL* values (T2 and T3) was generated when the entire residual stress balance was strongly disturbed by more complex and larger spike stresses due to the macroscopic and microscopic features of the xylem tissue. Notably, plank T4 showed a unique pattern, not bell-shaped, but a low *ISL* value, which requires further evaluation.

These characteristics were inferred to originate from the environmental factors such as ground inclination, surrounding trees, and climate conditions, which consequently affect the tree shape and distribution of tree structure, such as fibre and tension wood. These relationships were not confirmed in the present study, and further studies from both sides of the environment and the tissue structures are expected.

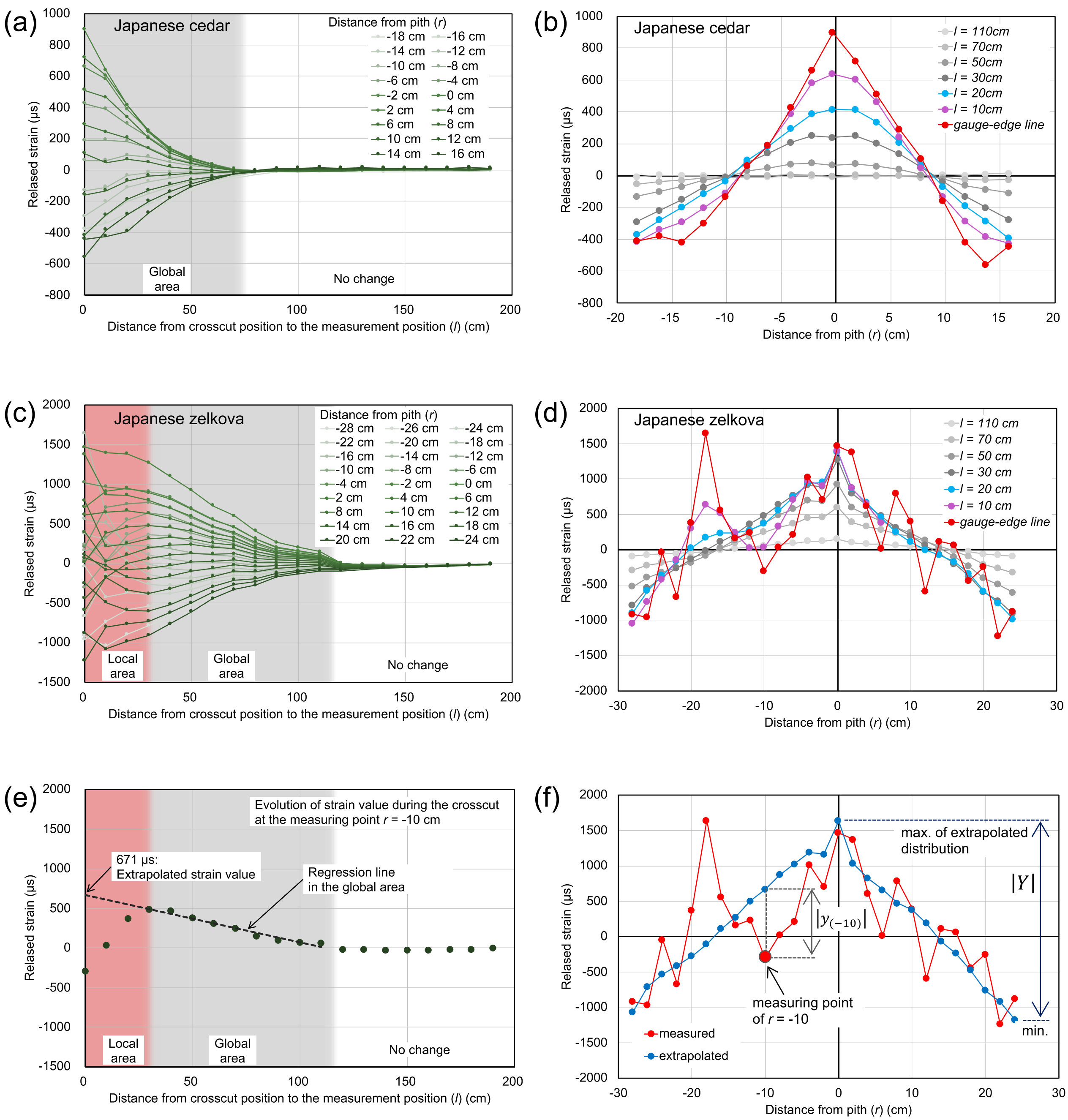

Fig. 5 Changes in released strain at each measurement point and released strain distribution: Comparison between Japanese cedar and zelkova. **a** Change in strain values of all strain gauges during crosscutting (Japanese cedar) (redrawn from [16]). **b** Change in released strain distribution during crosscutting (Japanese cedar) (redrawn from [16]). **c** Change in strain value of all strain gauges during crosscutting (Japanese zelkova) with the indication of local and global areas. **d** Change in released strain distribution during each crosscut (Japanese zelkova). **e** Extrapolation of the strain value toward the gauge-edge line ($l=0$ cm) from the linear regression in the global area. (Example of the measurement point at r=-10 cm). **f** Distributions of the measured strain at the gauge-edge line and extrapolated strain with the definitions of $|y(r)|$ and $|Y|$ to calculate $SL(r)$ and normalise the released strain. (Example of the measurement point at $r=-10$ cm)

Residual strain distribution at different longitudinal positions in log

In this final section, the spatial complexity of the distribution of the longitudinal released strain is discussed. Figure 7a–c shows the released strain distribution measured using two different logs from one tree, as shown in Fig. 1b, to verify the axial symmetry. For comparison, Fig. 7e shows the case of a large-diameter Japanese cedar

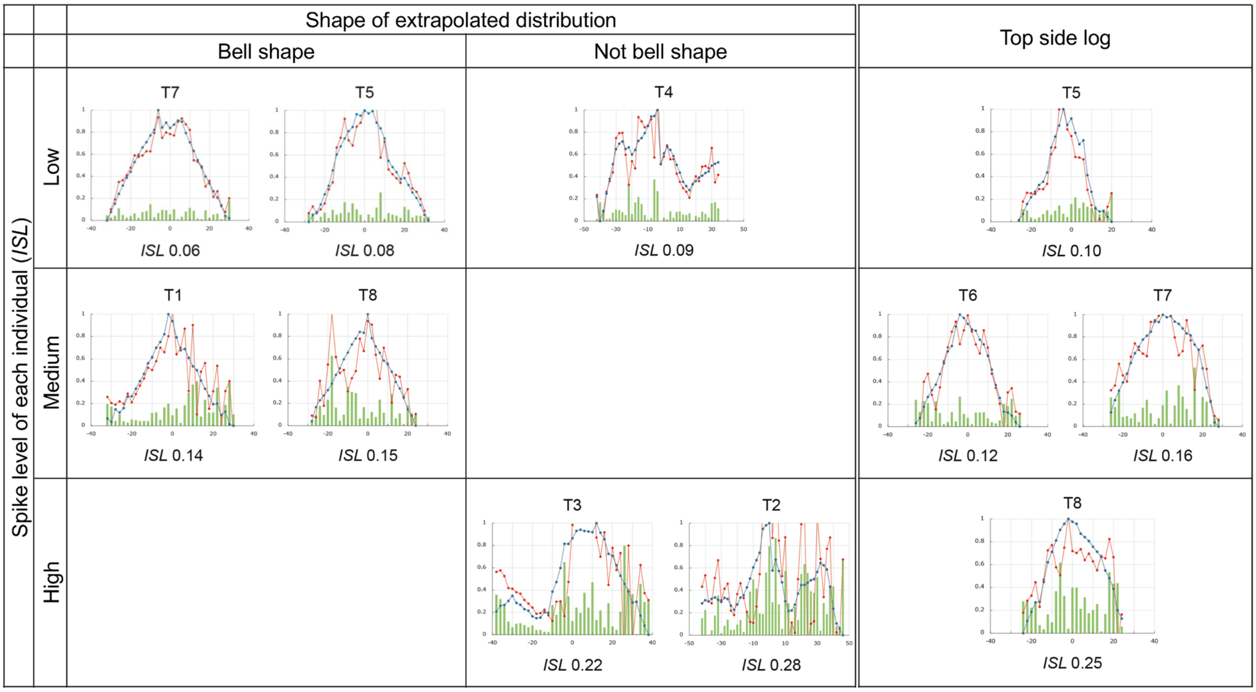

Fig. 6 Classification of the released strain distributions based on shape and *ISL* values. Graphs of distributions of the normalised measured strain (red points), extrapolated and normalised strain (blue points), and *SL*(*r*) values (green bars) were categorised based on the *ISL* values and shapes of the distribution. The top-side logs are also shown on the right column

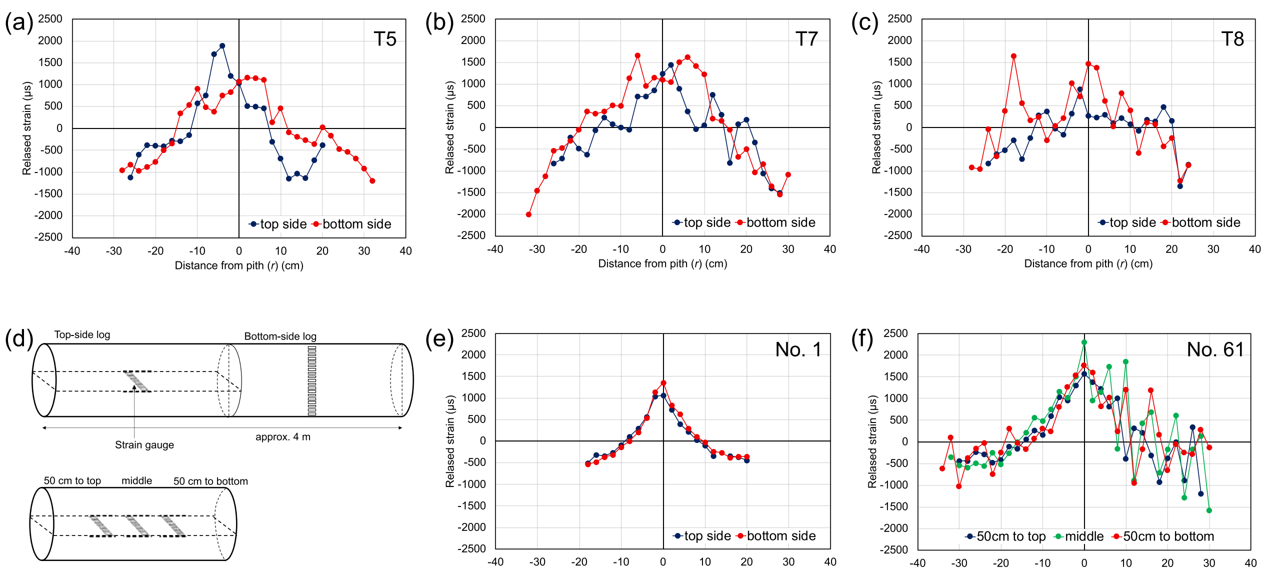

Fig. 7 Spatial symmetry of released strain distribution. (**a**), (**b**) and (**c**) Comparison of released strain distributions between top and bottom-side planks axially perpendicular to each other. (Sample T5, T7 and T8). (**d**) Illustration of measurement geometry in the previous reports. Upper: Japanese cedar for the released strain distribution shown in (**e**) [9]. Lower: Japanese zelkova for the distribution shown in (**f**) [4]. (**e**) Released strain distributions on top and bottom-side planks axially perpendicular to each other in a large-diameter Japanese cedar log (Sample No. 1 in [9]). (**f**) Released strain distributions at different longitudinal positions within the same plank of a large-diameter Japanese zelkova log (Sample No. 61 in [4])

with the sampling geometry shown in Fig. 7d (upper) [9], and Fig. 7d (lower) and 7f show the case of Japanese zelkova [4].

The characteristics of the distribution, such as frequency, intensity, and radial area, differed between the top and bottom-side logs, whose planes were perpendicular to each other (Fig. 7a–c). The distribution of the residual stress of Japanese cedar showed perfect axial symmetry around the pith (Fig. 7e). When the strain distribution was measured on the same plank of Japanese zelkova (Fig. 7f), the radial areas where the spike-shaped strain appeared were similar. Including the discussion in the previous sections, Japanese zelkova has a rather complex mechanism in the three-dimensional formation of the residual stress. The origin and the significance of this complexity are currently not clear. Further research, which should include other hardwood species of diffuse-porous wood and ring-porous wood with different annual ring widths, is needed to reveal the mechanisms behind the formation of such residual stress distributions, the advantages and disadvantages for the survival of trees, and the impacts of the unique distribution on wood utilisation.

Conclusion

The purpose of this study was to quantify the intensity of the spike-shaped strain that causes the unique distribution of released strain in large-diameter Japanese zelkova logs and to discuss the characteristics of that released strain. The spike-shaped strain and residual strain distributions were successfully quantified, which enabled comparisons among different logs. The detailed conclusions are as follows.

1. The released strain comprised two stress-state phases, named "local" and "global" areas.
2. The spike-shaped strain was quantified as the difference between the measured strain and a virtual baseline extrapolated from the global area.
3. The intensity of the spike strain was expressed as the individual spike levels, which varied widely among samples and appeared to relate to the overall shape of the strain distribution.
4. The residual stress distribution of large-diameter Japanese zelkova was not axially symmetric about the pith and exhibited three-dimensional complexity.

This study quantified the characteristic residual strain of Japanese zelkova, which exhibited features unique from those of ordinary wood species. The established method may provide a useful basis for understanding such species-specific stress formation and its possible implications for wood processing.

Abbreviations

μs Microstrain
SL Spike level
ISL Individual spike level

Acknowledgements

The authors are grateful to KAMEYAMA CONSTRUCTION Co., Ltd. for their support. The authors would like to thank Mr. Daizo Ishii for giving valuable knowledge on keyaki wood. The authors would also like to thank Mr. Masayuki Tomizuka for his assistance with data organisation and writing.

Author contributions

NK planned this study, conducted the experiments, analysed the data, and wrote the manuscript. MM-U co-supervised this study, conducted the experiments, analysed the data, and revised the manuscript. SC, JZ, JG, and FM-Y conducted experiments. MY co-supervised this study and provided specific advice. HY co-supervised this study, conducted the experiments and analyses, and revised the manuscript. All authors have read and approved the final manuscript.

Funding

This study was funded by JSPS KAKENHI Grant Number JP19H05360 (Grantin-Aid for Scientific Research on Innovative Areas, Elucidation of the strategies of mechanical optimisation in plants toward the establishment of the bases for sustainable structure system), Research Grant from Sakamoto Scholarship Foundation, the Kyoto University Foundation, and the Financial Support Program for the Employment of Research Assistants and Lab Assistants of Kyoto University.

Data availability

The datasets used and/or analysed during the current study are available from the corresponding author upon reasonable request.

Declarations

Competing interests

The authors declare that they have no competing interests.

Received: 8 August 2025 Accepted: 25 December 2025
Published online: 25 January 2026

References

1. Hashizume H, Furukawa I, Sakuno T, Omori H (1987) On the utilizing volume and wood quality of *Zelkova serrata* Makino. Hardwood Res 4:49–59 (In Japanese with English abstract)
2. Furukawa I, Fukutani S, Kishimoto J (1989) Characteristics of the variation of wood quality within keyaki (*Zelkova serrata*) trees -horizontal variations of ring width, fiber length, vessel element length, specific gravity and longitudinal compression strength. Hardwood Res 5:197–206 (In Japanese with English abstract)
3. Arioka T (2016) Keyaki. Hosei University Press, Tokyo (In Japanese)
4. Kameyama N, Matsuo-Ueda M, Cheng S, Jiang Z, Ichiyanagi T, Yoshida M, Yamamoto H (2023) Unique characteristics of residual stress distribution of large-diameter keyaki (*Zelkova serrata*) logs and examination of their measurement method. J Wood Sci 69:16
5. Archer RR (1987) Growth stresses and strains in trees. Springer, Berlin Heidelberg
6. Jacobs MR (1945) The growth stresses of woody stems. Commonw Aust For Timber Bur Bull 28:1–67
7. Nikolov SV, Videlov HR, Evitimov G, Yosifov B (1967) Biological internal stresses in wood of beech (*Fagus silvatica* L.). For Univ, Sofia, Sci Works, Series Mech Technol Wood 15: 21–31
8. Saurat J, Guéneau P (1976) Growth stresses in beech. Wood Sci Technol 10:111–123
9. Matsuo-Ueda M, Tsunezumi T, Jiang Z, Yoshida M, Yamashita K, Matsuda Y, Matsumura Y, Ikami Y, Yamamoto H (2022) Comprehensive study of

distributions of residual stress and Young's modulus in large-diameter sugi (*Cryptomeria japonica*) log. Wood Sci Tech 56:573–588

10. Watanabe H (1967) A study of the origin of longitudinal growth stresses in tree stems. Bull Kyushu Univ For 41:169–176 (In Japanese with English abstract)
11. Okuyama T, Kanagawa Y, Hattori Y (1987) Reduction of residual stresses in logs by direct heating method. Mokuzai Gakkaishi 33:837–843
12. Okuyama T, Yamamoto H (1992) Residual stresses in living tree. In: Fujiwara H, Abe T, Tanaka K (eds) Residual stresses - III. Science and Technology. Elsevier Applied Science, London and New York, pp 128–133.
13. Wahyudi I, Okuyama T, Sudo-Hadi Y, Yamamoto H, Yoshida M, Watanabe H (1999) Growth stress and strains in *Acacia mangium*. For Prod J 49(2):77–81
14. Wahyudi I, Okuyama T, Sudo-Hadi Y, Yamamoto H, Yoshida M, Watanabe H (2000) Relationship between growth rate and growth stresses in *Paraserianthes falcataria* grown in Indonesia. J Trop For Prod 6:95–105
15. Wahyudi I, Okuyama T, Sudo-Hadi Y, Yamamoto H, Watanabe H, Yoshida M (2001) Relationship between released strain and growth rate in 39 year-old *Tectona grandis* planted in Indonesia. Holzforschung 55:63–66
16. Yamashita K, Kato H, Matsuo-Ueda M, Yamamoto H (2021) Measurement of residual stress in large-diameter sugi (*Cryptomeria japonica*) log using boards with pith. Wood industry 76 (11): 462–467 (In Japanese with English abstract)

Publisher's Note